



OPEN Validation of a motion model for soccer players' sprint by means of tracking data

Takuma Narizuka^{1✉}, Kenta Takizawa² & Yoshihiro Yamazaki³

In soccer game analysis, the widespread availability of play-by-play and tracking data has made it possible to test mathematical models that have been discussed mainly theoretically. One of the essential models in soccer game analysis is a motion model that predicts the arrival point of a player in t s. Although many space evaluation and pass prediction methods rely on motion models, the validity of each has not been fully clarified. This study focuses on the motion model proposed by Fujimura and Sugihara (Fujimura–Sugihara model) under sprint conditions based on the equation of motion. A previous study indicated that the Fujimura–Sugihara model is ineffective for soccer games because it generates a circular arrival region. This study aims to examine the validity of the Fujimura–Sugihara model using soccer tracking data. Specifically, we quantitatively compare the arrival regions of players between the model and real data. We show that the boundary of the player's arrival region is circular rather than elliptical, which is consistent with the model. We also show that the initial speed dependence of the arrival region satisfies the solution of the model. Furthermore, we propose a method for estimating valid kinetic parameters in the model directly from tracking data and discuss the limitations of the model for soccer games based on the estimated parameters.

Over the past decade, various types of data have become available for sports data analysis. In particular, the prevalence of play-by-play¹ and tracking data² for soccer games has enabled new analyses that were previously impossible³. Some typical examples include ball-passing network analysis^{4,5}, formation analysis^{6,7}, and space evaluation^{8–10}. Such research topics require a variety of statistical analysis methods, including network theory, computational geometry, and machine learning. In particular, machine learning is an effective tool for soccer game analysis because soccer produces very complex behaviors from simple unified rules and has a huge accumulation of data. Soccer games are a good laboratory to develop cutting-edge machine learning techniques^{11,12}.

Statistical properties of player interactions and collective motions are also hot topics in soccer game analysis. In terms of statistical physics, soccer players can be regarded as self-propelled particles¹³. We can apply some techniques developed for characterizing the self-propelled particles, including flocks of birds or fish schools¹⁴. The examples include the detection of highly correlated segments using directional correlation functions¹⁵, the characterization of order-disorder transition¹⁶, and the modeling of soccer players' motion by the self-propelled player model¹⁷. Furthermore, the dynamics of player interactions and ball passing in soccer games are described as stochastic processes, such as the Markov chain¹⁸ and the first-passage process¹⁹.

The widespread use of these new data has also made it possible to test mathematical models that have mainly been discussed theoretically in soccer game analysis. One of the essential models in soccer games is a motion model, which calculates the arrival point of a player in t s based on the current location and velocity. The two practical applications of motion models in soccer games are space evaluation and pass prediction. In space evaluation, a fundamental concept is the “dominant region,” defined as the region where a specific player can arrive before other players^{3,20}. In general, we can estimate the dominant region of each player by comparing the arrival times of all players to each location in the field. In addition, the outcome of a given pass can be estimated by calculating the arrival time of each player on the ball trajectory^{17,21–23}. Because the motion model can calculate the arrival times of a player to a specific location, it is essential for soccer game analysis.

Thus far, various motion models have been proposed. The simplest motion model assumes uniform linear motion for all players, resulting in the Voronoi region as the dominant region. More realistic models have also been proposed; for example, Taki and Hasegawa assumed uniform accelerated motion of players^{20,24}, and

¹Faculty of Data Science, Risho University, Kumagaya, Saitama 360-0194, Japan. ²Department of Physics, Faculty of Science and Engineering, Chuo University, Bunkyo, Tokyo 112-8551, Japan. ³Department of Physics, School of Advanced Science and Engineering, Waseda University, Shinjuku, Tokyo 169-8555, Japan. ✉email: pararel@gmail.com

Fujimura and Sugihara considered viscous resistance²¹. These motion models are based on the equation of motion and are often referred to as the “physics-based motion model.” They provide the arrival points of players under specific conditions such that each player moves to all locations by sprinting.

Another type of motion model calculates the arrival points of players based on machine learning^{25–27}. This “probabilistic motion model” can predict realistic arrival points based on previous tracking data, though it is costly for learning. We note that because the tracking data used for learning include various running patterns other than a sprint, the predicted arrival point does not necessarily mean the position arrived by sprinting.

Both physics-based motion models and probabilistic motion models aim to predict the arrival point of players. Physics-based motion models also play a role in elucidating the principles of players’ movement laws. This study focuses on the motion model proposed by Fujimura and Sugihara (hereinafter Fujimura–Sugihara model) in sprint conditions to elucidate soccer players’ movement laws during sprinting. Specifically, we aim to investigate the validity and limitations of the Fujimura–Sugihara model based on soccer tracking data. We stress that the motion model in the sprint condition is significant in situations where we calculate the minimum arrival time of players to each location. The minimum arrival time is utilized to evaluate which player can receive the ball^{21,22} and to quantify the degree of safety and sparsity of each location in the field¹⁰. Thus, the present study provides an essential basis for various applied analyses.

In our investigation, we first focused on the shape of the arrival region of players predicted by the motion model. The Fujimura–Sugihara model generates a circular arrival region²¹. However, it has been pointed out that the arrival region should be elliptical, considering the difference in the acceleration ability of players depending on the direction of motion^{8,26}. We show that the circular arrival region is obtained from soccer tracking data, and the arrival region’s initial speed dependence also satisfies the Fujimura–Sugihara model’s solution. Next, we propose a method to estimate the kinetic parameters of the Fujimura–Sugihara model. Contrary to previous experiment-based methods²¹, this method can estimate valid parameters directly from tracking data. Finally, we discuss the limitations of the Fujimura–Sugihara model for soccer games based on the time dependence of the estimated kinetic parameters.

Method

Data. The datasets used in this study were from 54 soccer games in the top division of the Japan Professional Football League (J1 League). Each game was played by 18 teams in 2016. The primary data of our dataset is absolute positional coordinates (x, y) of all players every 0.04 s, collected by using the TRACAB system²⁸. The x and y coordinates are considered to contain an error of ± 1 m by assessing the accuracy of the TRACAB system. These datasets were provided by DataStadium Inc., Japan, which was authorized to collect and sell these data under a contract with the J League²⁹. This contract also ensures that the use of relevant datasets does not infringe on the rights of players and clubs belonging to the J League. Although the datasets were proprietary, we received explicit permission from DataStadium Inc. for use in this study. This study’s Data analyses and visualizations were performed using Python packages on an iMac Pro system with a 3-GHz 10-Core Intel Xeon W processor and 128 GB of memory.

Preliminary analysis. We summarize the basic properties of soccer players’ motions. The player’s velocity $\vec{v}(t)$ was calculated as the difference between the current position and the position 1 s ago. Figure 1a shows the speed distributions for the goalkeeper and the other players obtained from a game. It is found that all players have a peak at $v \simeq 1$ m/s, whereas the non-goalkeepers have a second peak at $v \simeq 3$ m/s. These two peaks correspond to walking and jogging, respectively. Figure 1b shows that the speed distribution of the non-goalkeepers is more widely distributed than that of the goalkeeper, and both decay almost exponentially. Because the sprint is observed mainly for players other than the goalkeeper, we exclude goalkeepers in the following analysis.

We also examine mean squared displacement (MSD) to characterize players’ trajectories. When a player at location $\vec{x}(t)$ at t moves to location $\vec{x}(t + \tau)$ after τ [s], MSD is defined as $\langle |\Delta\vec{x}|^2 \rangle_\tau = \langle |\vec{x}(t + \tau) - \vec{x}(t)|^2 \rangle_\tau$. In general, MSD is scaled as

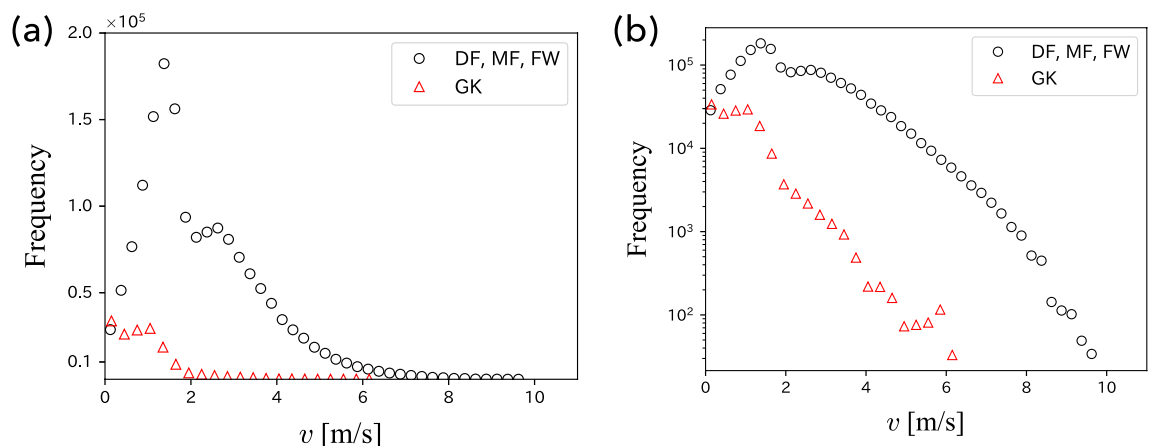


Figure 1. Speed distributions of soccer players. (a) Linear plot and (b) semi-logarithmic plot.

$$\langle |\Delta \vec{x}|^2 \rangle_\tau \sim \tau^\beta, \tag{1}$$

where the exponent β reflects the trajectory of the player; in particular, $\beta = 1$ and 2 correspond to the simple random walk and linear motion of the player, respectively. In real data analysis, we calculated MSD for a player as the long-time average defined as follows:

$$\langle |\Delta \vec{x}|^2 \rangle_\tau = \frac{1}{T - \tau} \sum_{t=0}^{T-\tau} |\vec{x}(t + \tau) - \vec{x}(t)|^2, \tag{2}$$

where T is the length of a single time series from a restart to a time-out in a game. In Fig. 2, we present the τ dependence of MSD obtained from the entire time series in a game; each line in Fig. 2 is obtained by averaging MSD over all players except for the goalkeeper. It is found that each line exhibits $\beta = 2$ in $\tau \lesssim 10$ s and $\beta = 1$ in $\tau \gtrsim 10$ s. This result indicates that each player moves in a straight line for up to 10 s and then changes direction randomly. Thus, the physics-based deterministic motion model is considered valid for a range of up to 10 s.

Fujimura–Sugihara model. We summarize the motion model proposed by Fujimura and Sugihara²¹. For the position $\vec{x}(t)$ of a player at time t , the Fujimura–Sugihara model is given by the following equation of motion:

$$m \frac{d^2 \vec{x}(t)}{dt^2} = F \vec{n} - k \frac{d\vec{x}(t)}{dt}, \tag{3}$$

where m is the mass of the player, F and \vec{n} are the magnitude and direction of the driving force, respectively, and k is the coefficient of viscous resistance. In other words, the player accelerates in the direction of \vec{n} with a magnitude F , and it becomes harder to accelerate in proportion to its velocity $d\vec{x}(t)/dt$. Given an initial position $\vec{x}_0 = (0, 0)$ and an initial velocity \vec{v}_0 , the solution is given as follows:

$$\vec{x}(t) = \frac{1 - \exp(-\alpha t)}{\alpha} \vec{v}_0 + V_{\max} \left(t - \frac{1 - \exp(-\alpha t)}{\alpha} \right) \vec{n}, \tag{4}$$

where $V_{\max} = F/k$ and $\alpha = k/m$ are arbitrary constants referred to as “kinetic parameters.” Here, we define the first and second coefficients in Eq. (4) as

$$A(\alpha, t) = \frac{1 - \exp(-\alpha t)}{\alpha}, \tag{5}$$

$$B(\alpha, V_{\max}, t) = V_{\max} \left(t - \frac{1 - \exp(-\alpha t)}{\alpha} \right) = V_{\max} (t - A(\alpha, t)). \tag{6}$$

When the direction of the driving force \vec{n} changes arbitrarily, the arrival points in t [s] of the player are distributed on a circle with center $A(\alpha, t)\vec{v}_0$ and radius $B(\alpha, V_{\max}, t)$; this circle is referred to as “arrival circle” hereinafter. Fujimura and Sugihara conducted a sprint experiment with three amateur hockey players to estimate the kinetic parameters. By fitting the obtained speed curve with the solution of the Fujimura–Sugihara model, they empirically obtained the kinematic parameters $V_{\max} = 7.8$ m/s and $\alpha = 1.3$ 1/s as the typical values during sprinting²¹.

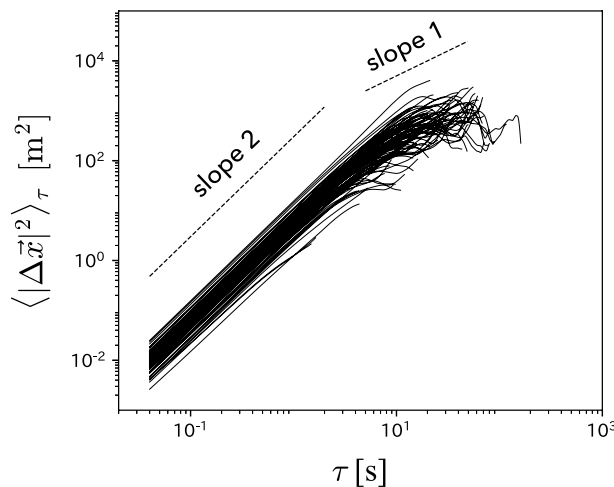


Figure 2. τ dependence of the mean squared displacement of soccer players. The graph is shown in double logarithmic scale.

Investigation method. To characterize the arrival points of players in Δt [s] using tracking data, we adopt the method used in previous studies^{21,26}. First, the velocity $\vec{v}(t)$ of each player at time t is converted to start at the origin (0, 0) and point in the positive direction of the x axis (Fig. 3). We then plot the location of the same player at $t + \Delta t$ on the same coordinates. By repeating this plot for various players and t , we obtain a heat map formed by the arrival points in Δt [s].

The shape of the heat map reflects the movement pattern of each player during Δt . For example, when players lose speed during Δt , they arrive at a point within the heat map. However, they arrived at a point around the boundary in the case of sprinting. Because we investigated the validity of the Fujimura–Sugihara model under sprint conditions, we focused on the shape of the heat map's boundary and compared it with the solution (4). We set $\vec{v}_0 = (v_0, 0)$, where $v_0 > 0$, in Eq. (4) for comparison with the heat map.

In the following analyses, we calculated heat maps using all data during the playing time of 54 games for all players except the goalkeepers. The controlling parameters were the initial speed v_0 [m/s] and time interval Δt [s]. Specifically, for a fixed Δt , we calculated the heat maps for the initial speed $[v_0, v_0 + \Delta v_0]$, where $\Delta v_0 = 0.3$ m/s ($\simeq 1$ km/h). We set one cell side in the heat map to $0.2 \times \Delta t$ [m], and only cells adjacent to more than c nonblank cells were used for the analyses. To exclude isolated cells as outliers, we manually set the value of c to eight for $\Delta t < 1$, six for $1 \leq \Delta t \leq 3$, and four for $3 < \Delta t$.

Result

v_0 dependence of heat map. Figure 4a,b present the heat maps of the players' arrival points for various initial speeds, $v_0 = 1, 3, 5, 7$ m/s, where $\Delta t = 1$ and 2 s. We focused only on the shape of each heat map's boundary, although the color gradation of the heat map is proportional to the number of data points. Remarkably, Fig. 4a,b show that the boundary of the heat map is not elliptical but circular for any initial v_0 . This result is consistent with the solution (4) of the Fujimura–Sugihara model.

Next, we approximated the boundary of each heat map as a circle and estimated its center coordinates (x_c, y_c) and radius r_c . After excluding the isolated heatmap cells as outliers, we calculated the maximum and minimum values of the heat maps x and y coordinates, x_{\max} , x_{\min} , y_{\max} , and y_{\min} . Then, (x_c, y_c) and r_c were estimated as follows:

$$(x_c, y_c) = \left(\frac{x_{\max} + x_{\min}}{2}, \frac{y_{\max} + y_{\min}}{2} \right), \quad (7)$$

$$r_c = \frac{x_{\max} - x_{\min} + y_{\max} - y_{\min}}{4}. \quad (8)$$

Figure 5 shows the v_0 dependence of x_c and y_c . We find that y_c is independent of v_0 ; namely, $y_c \simeq 0$. However, x_c is proportional to v_0 , particularly for $v_0 \lesssim 6$ m/s. The dotted lines in each panel of Fig. 5 represent the regression line for the points where $v_0 \leq 6$ m/s. These results are consistent with the solution (4) of the Fujimura–Sugihara model.

We also examined the v_0 dependence of the radius r_c of the estimated circle. Figure 6 shows that r_c becomes almost constant, particularly for $v_0 \lesssim 6$ m/s. The dotted line in each panel of Fig. 6 represents the average value of r_c where $v_0 \leq 6$ m/s. As $B(\alpha, V_{\max}, t)$ in Eq. (4) is independent of v_0 , this result is also consistent with the solution (4) of Fujimura–Sugihara model.

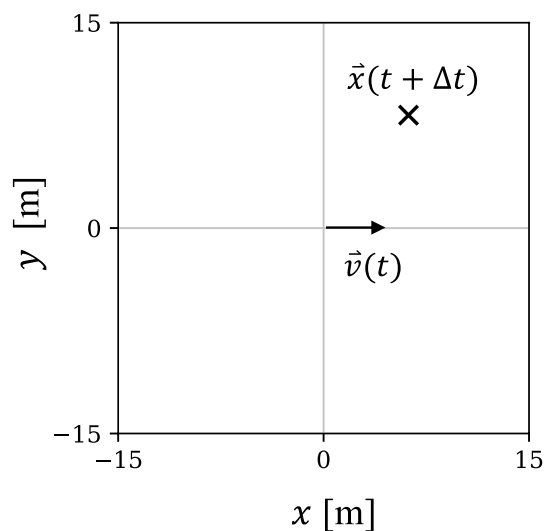


Figure 3. Coordinate system for the calculation of heat maps.

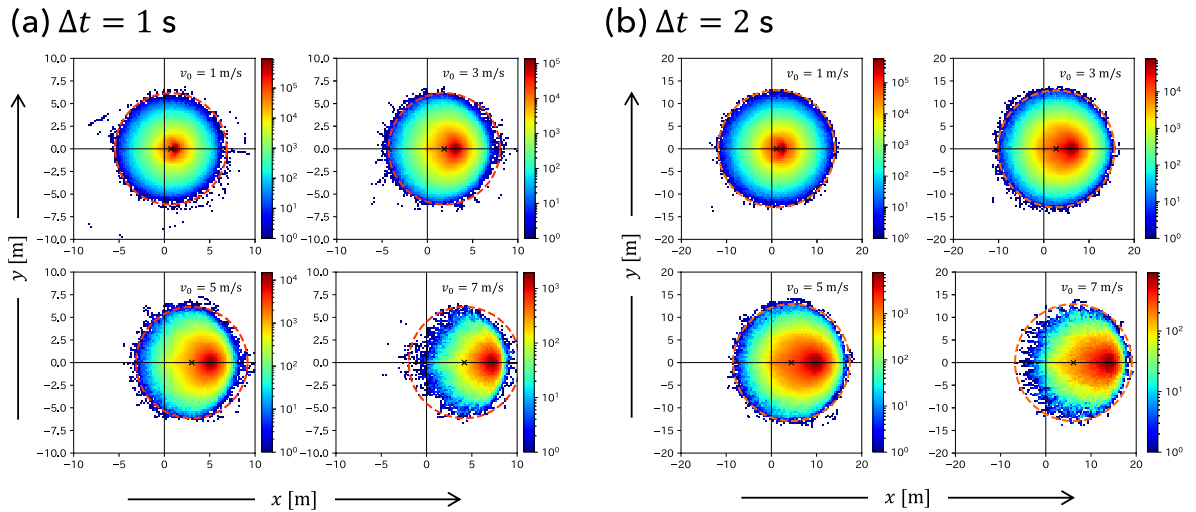


Figure 4. Heat maps of players' arrival points for various initial speed $v_0 = 1, 3, 5, 7$ m/s, where (a) $\Delta t = 1$ s and (b) $\Delta t = 2$ s. The dotted line in each panel represents the arrival circle (4) with kinetic parameters estimated from the heat maps.

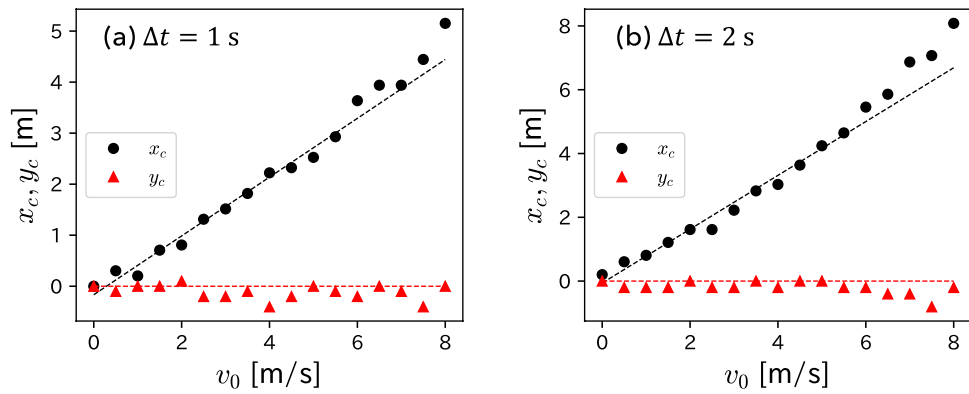


Figure 5. v_0 dependence of the center coordinates x_c and y_c of the estimated circle of each heat map, where (a) $\Delta t = 1$ s and (b) $\Delta t = 2$ s. The dotted lines in each panel represent the regression line for points where $v_0 \leq 6$ m/s.

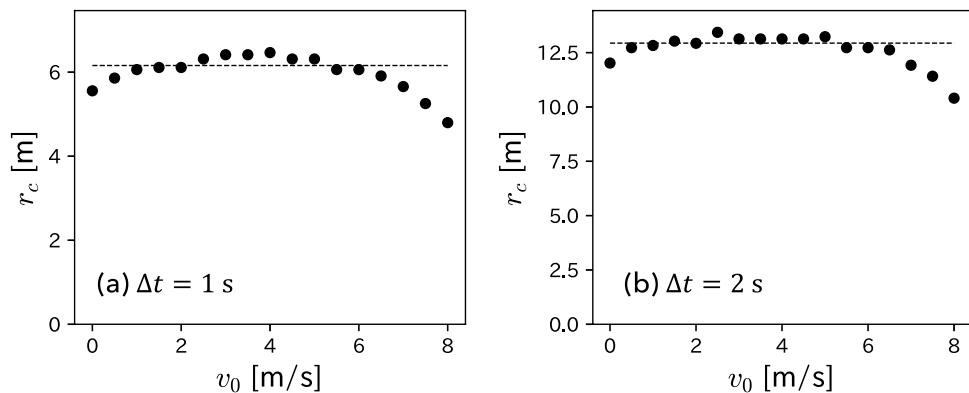


Figure 6. v_0 dependence of the radius r_c of the estimated circle of each heat map. The dotted line represents $r_c = 6.16$ m for (a) $\Delta t = 1$ s, and $r_c = 12.94$ m for (b) $\Delta t = 2$ s. These values are obtained by averaging the points where $v_0 \leq 6$ m/s.

Estimation of kinetic parameters using heat maps. According to the solution (4), the x coordinate of the arrival circle is proportional to v_0 , and the proportionality coefficient is given by Eq. (5). Because we obtained the result that x_c calculated from the heat map is proportional to v_0 (refer to Fig. 5), we can estimate the kinetic parameter α using Eq. (5). Specifically, the proportionality coefficients obtained from the regression line shown in Fig. 5a,b are 0.58 and 0.84; then, we obtain $\alpha = 1.23$ and 1.04 1/s for $\Delta t = 1$ and 2 s, respectively.

The radius of the arrival circle is given by Eq. (6). As shown in Fig. 6a,b, the radius of the estimated circle of each heat map has become $r_c \simeq 6.16$ and 12.94 m for $\Delta t = 1$ and 2 s. Thus, the estimated values of α and Eq. (6) can yield another kinetic parameter V_{\max} ; we obtain $V_{\max} = 14.53$ and 11.19 m/s, respectively.

The dotted lines in each panel of Fig. 4 show the arrival circle calculated by the solution (4) with the above estimated kinetic parameters α and V_{\max} . We found that the solution (4) of the Fujimura–Sugihara model can correctly predict the boundary of the arrival region.

Δt dependence of kinetic parameters. We also analyze the dependence of the kinetic parameters on Δt . As a result of the same analyses in the previous section for different Δt , we confirm the characteristics shown in Figs. 4, 5, and 6 for all Δt . We present the Δt dependence of the estimated kinetic parameters in Fig. 7. Although α and V_{\max} are assumed to be constant in the Fujimura–Sugihara model, we found that the estimated kinetic parameters vary with Δt , particularly in the range of $\Delta t \lesssim 1$ s.

Discussion and conclusion

We investigated the validity of the Fujimura–Sugihara model based on heat maps of the players' arrival points obtained from soccer tracking data. Our results can be summarized as follows. First, the boundary of the heat map became a circle rather than an ellipse. Second, x_c was proportional to v_0 and y_c was independent of v_0 . Third, r_c was independent of v_0 . These results are consistent with the solution (4) of the Fujimura–Sugihara model. We also proposed a method for estimating valid kinetic parameters in the Fujimura–Sugihara model. Meanwhile, the estimated kinetic parameters varied with Δt , particularly in $\Delta t \lesssim 1$ s; this result is inconsistent with the assumption of the Fujimura–Sugihara model.

In the previous study by Fujimura and Sugihara, the kinetic parameters were estimated by a sprint experiment²¹. The experiment subjects were members of a college field hockey team who ran in a straight line by sprinting. They empirically obtained the kinetic parameters $\alpha = 1.3$ 1/s and $V_{\max} = 7.8$ m/s by fitting the solution of the Fujimura–Sugihara model to the speed curve of each subject. In the present study, we estimated the parameters based on each soccer player's real positional data. The obtained values were slightly different from the previous study; for example, $\alpha = 1.04$ 1/s and $V_{\max} = 11.19$ m/s for $\Delta t = 2$ s. However, our estimation method of kinetic parameters is more reasonable than the previous empirical one in the sense that the parameters were estimated directly from the soccer tracking data.

Note that as shown in Figs. 4, 5, and 6, the plot in large v_0 region is different from the others. This discrepancy is because of the few data points of the heat maps in the large v_0 region. For example, a player with large v_0 is unlikely to move in the opposite direction during Δt . Namely, the larger the v_0 , the fewer the data points in the region $x < 0$ in the heat maps. The estimated values of (x_c, y_c) and r_c for large v_0 values appear to be incorrect because they are calculated using the maximum and minimum values of the heat maps x and y coordinates. In the future, the use of large-scale tracking data could eliminate such problems.

We comment on the results of the Δt dependence of the kinetic parameters shown in Fig. 7. This result requires careful consideration from two perspectives. First, the x and y coordinates of our tracking data contain an error of ± 1 m by assessing the accuracy of the TRACAB system. This error cannot be ignored in the analysis of the heat maps, especially when $\Delta t \lesssim 1$ s. Therefore, we must check the validity of the rapid increase in α and V_{\max} in Fig. 7 using more accurate data. The second possibility is that the results in Fig. 7 indicate the limitation of the Fujimura–Sugihara model. The Fujimura–Sugihara model must be extended to reproduce the behavior shown in Fig. 7. One possible extension is a model in which the magnitudes of the driving force F and viscous resistance k in Eq. (3) are time-dependent:

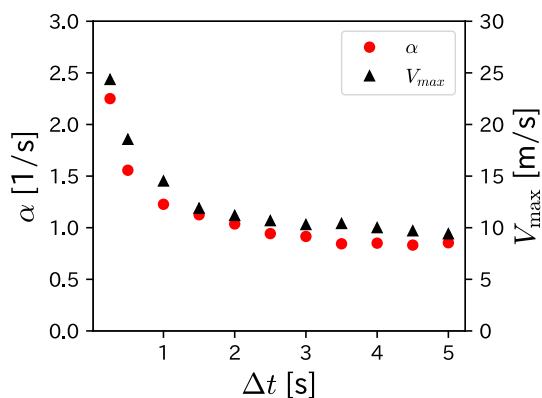


Figure 7. Δt dependence of kinetic parameters, α and V_{\max} .

$$m \frac{d^2 \vec{x}(t)}{dt^2} = F(t) \vec{n} - k(t) \frac{d\vec{x}(t)}{dt}. \quad (9)$$

This equation is known as the variable coefficient second-order linear ODE. As the time dependence of kinetic parameters is conceivable in soccer, the analysis of this extended motion model can be a challenging and significant future topic in soccer game analysis.

Previously, Brefeld et al. demonstrated that the arrival region of soccer players becomes elliptical²⁶. Fernández et al. modeled the player influence area as elliptical when the initial speed is large⁸. However, Anzer et al. pointed out that the smaller the speed interval Δv_0 , the closer the shape of the arrival region is to be circular rather than elliptical²³. This study supports the results of Anzer et al. with a more detailed and comprehensive analysis. Furthermore, we have recently shown that soccer players' sprints satisfy the characteristics of the Fujimura–Sugihara model, that is, v_0 dependence of the arrival circle for fixed Δt . Our results suggest that a relatively simple model can describe soccer players' sprints, although a slight discrepancy exists between actual observations and model predictions. Furthermore, the motion model under the sprint condition was utilized for pass prediction^{17,21,22} and for modeling the dominance and influence of soccer players at each location in the field¹⁰. Our observations are fundamental characteristics that the motion model should satisfy and provide direction for modeling soccer players' motions.

In conclusion, the Fujimura–Sugihara model effectively predicts the arrival point of soccer players by sprinting, except when the time interval Δt is small. The boundary of the player's arrival region is shown to be circular rather than elliptical; the initial speed dependence of the arrival region satisfies the model. In the case of sprinting, kinetic parameters in the model can be estimated directly from the soccer tracking data.

Data availability

The dataset (Player Tracking Data in J-League Matches) was obtained from DataStadium Inc., Japan. It is not publicly available, but it was provided to us based on an agreement with the company. The dataset is however available from the corresponding author (T. Narizuka) upon reasonable request and with permission of DataStadium.

Received: 12 April 2022; Accepted: 11 January 2023

Published online: 17 January 2023

References

- Pappalardo, L. et al. A public data set of spatio-temporal match events in soccer competitions. *Sci. Data* **6**, 236 (2019).
- Pettersen, S. A. et al. Soccer video and player position dataset. in *Proceedings of the 5th ACM Multimedia Systems Conference*. 18–23 (2014).
- Gudmundsson, J. & Horton, M. Spatio-temporal analysis of team sports. *ACM Comput. Surv.* **50**, 1–42 (2017).
- Duch, J., Waitzman, J. S. & Amaral, L. A. N. Quantifying the performance of individual players in a team activity. *PLoS ONE* **5**, e10937 (2010).
- Buldú, J. M., Busquets, J., Echegoyen, I. & Seirullo, F. Defining a historic football team: Using network science to analyze Guardiola's F.C. Barcelona. *Sci. Rep.* **9**, 1–14 (2019).
- Bialkowski, A. et al. Large-scale analysis of soccer matches using spatiotemporal tracking data. in *2014 IEEE International Conference on Data Mining*. 725–730 (2014).
- Narizuka, T. & Yamazaki, Y. Clustering algorithm for formations in football games. *Sci. Rep.* **9**, 1–8 (2019).
- Fernández, J. & Bornn, L. Wide open spaces : A statistical technique for measuring space creation in professional soccer. in *Proceedings of the MIT Sloan Sports Analytics Conference*. 1–19 (2018).
- Spearman, W. Beyond expected goals. in *Proceedings of the MIT Sloan Sports Analytics Conference*. 1–17 (2018).
- Narizuka, T., Yamazaki, Y. & Takizawa, K. Space evaluation in football games via field weighting based on tracking data. *Sci. Rep.* **11**, 1–8 (2021).
- Kurach, K. et al. Google research football: A novel reinforcement learning environment. *Proc. AAAI Conf. Artif. Intell.* **34**, 4501–4510 (2020).
- Tuyls, K. et al. Game plan: What AI can do for football, and what football can do for AI. *J. Artif. Intell. Res.* **71**, 41–88 (2021).
- Sumpter, D. *Soccermatics: Mathematical Adventures in the Beautiful Game* (Bloomsbury Sigma, 2016).
- Vicsek, T. & Zafeiris, A. Collective motion. *Phys. Rep.* **517**, 71–140 (2012).
- Marcelino, R. et al. Collective movement analysis reveals coordination tactics of team players in football matches. *Chaos Solit. Fractals* **138**, 109831 (2020).
- Narizuka, T. & Yamazaki, Y. Statistical properties for directional alignment and chasing of players in football games. *Europhys. Lett.* **116**, 68001 (2017).
- Alguacil, F. P., Fernández, J. & Arce, P. P. Seeing in to the future : Using self-propelled particle models to aid player decision-making in soccer. in *Proceedings of the MIT Sloan Sports Analytics Conference*. 1–23 (2020).
- Narizuka, T., Yamamoto, K. & Yamazaki, Y. Statistical properties of position-dependent ball-passing networks in football games. *Physica A* **412**, 157–168 (2014).
- Chacoma, A., Almeida, N., Perotti, J. I. & Billoni, O. V. Modeling ball possession dynamics in the game of football. *Phys. Rev. E* **102**, 042120 (2020).
- Taki, T. & Hasegawa, J.-I. Visualization of dominant region in team games and its application to teamwork analysis. *Proc. Comput. Graph. Int.* **2000**, 227–235 (2000).
- Fujimura, A. & Sugihara, K. Geometric analysis and quantitative evaluation of sport teamwork. *Syst. Comput. Jpn.* **36**, 49–58 (2005).
- Spearman, W., Basye, A., Dick, G., Hotovy, R. & Pop, P. Physics-based modeling of pass probabilities in soccer. in *Proceedings of the MIT Sloan Sports Analytics Conference*. 1–14 (2017).
- Anzer, G. & Bauer, P. Expected passes. *Data Min. Knowl. Discov.* 1–23 (2022).
- Taki, T., Hasegawa, J.-I. & Fukumura, T. Development of motion analysis system for quantitative evaluation of teamwork in soccer games. in *Proceedings of 3rd IEEE International Conference on Image Processing*. Vol. 3. 815–818 (1996).
- Gudmundsson, J. & Wolle, T. Football analysis using spatio-temporal tools. *Comput. Environ. Urban Syst.* **47**, 16–27 (2014).
- Brefeld, U., Lasek, J. & Mair, S. Probabilistic movement models and zones of control. *Mach. Learn.* **108**, 127–147 (2019).
- Caetano, F. G. et al. Football player dominant region determined by a novel model based on instantaneous kinematics variables. *Sci. Rep.* **11**, 1–10 (2021).
- Tracab Technologies. <https://tracab.com/products/tracab-technologies/>. Accessed 9 Feb 2022 (2022).

29. DataStadium Inc. <https://www.datastadium.co.jp/en/index>. Accessed 9 Feb 2022.

Acknowledgements

The authors are grateful to DataStadium Inc., Japan, for providing the player tracking data for this study. This work was partially supported by the Data-Centric Science Research Commons Project of the Research Organization of Information and Systems, Japan, a Grant-in-Aid for Young Scientists (18K18013) from the Japan Society for the Promotion of Science (JSPS), and Hayao Nakayama Foundation for Science and Technology and Culture (22-KI-09).

Author contributions

T.N. and K.T. designed the study and performed the analyses. Y.Y. supervised the study and proposed the direction for the analyses. T.N. prepared the manuscript, while Y.Y. critically reviewed it. All authors discussed the results and approved the final manuscript.

Competing interests

The authors declare no competing interests.

Additional information

Correspondence and requests for materials should be addressed to T.N.

Reprints and permissions information is available at www.nature.com/reprints.

Publisher's note Springer Nature remains neutral with regard to jurisdictional claims in published maps and institutional affiliations.



Open Access This article is licensed under a Creative Commons Attribution 4.0 International License, which permits use, sharing, adaptation, distribution and reproduction in any medium or format, as long as you give appropriate credit to the original author(s) and the source, provide a link to the Creative Commons licence, and indicate if changes were made. The images or other third party material in this article are included in the article's Creative Commons licence, unless indicated otherwise in a credit line to the material. If material is not included in the article's Creative Commons licence and your intended use is not permitted by statutory regulation or exceeds the permitted use, you will need to obtain permission directly from the copyright holder. To view a copy of this licence, visit <http://creativecommons.org/licenses/by/4.0/>.

© The Author(s) 2023